

PCCP

Accepted Manuscript



This is an *Accepted Manuscript*, which has been through the Royal Society of Chemistry peer review process and has been accepted for publication.

Accepted Manuscripts are published online shortly after acceptance, before technical editing, formatting and proof reading. Using this free service, authors can make their results available to the community, in citable form, before we publish the edited article. We will replace this *Accepted Manuscript* with the edited and formatted *Advance Article* as soon as it is available.

You can find more information about *Accepted Manuscripts* in the [Information for Authors](#).

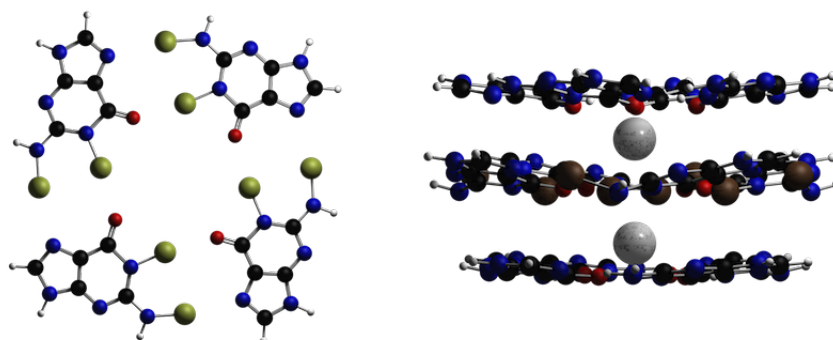
Please note that technical editing may introduce minor changes to the text and/or graphics, which may alter content. The journal's standard [Terms & Conditions](#) and the [Ethical guidelines](#) still apply. In no event shall the Royal Society of Chemistry be held responsible for any errors or omissions in this *Accepted Manuscript* or any consequences arising from the use of any information it contains.

Covalency in Resonance-Assisted Halogen Bonds Demonstrated with Cooperativity in *N*-Halo-Guanine Quartets

Lando P. Wolters, Nicole W. G. Smits, Célia Fonseca Guerra*

Department of Theoretical Chemistry and Amsterdam Center for Multiscale Modeling,
VU University Amsterdam, De Boelelaan 1083, 1081 HV Amsterdam (The Netherlands).

E-mail: c.fonseca Guerra@vu.nl



Abstract

Halogen bonds are shown to possess the same characteristics as hydrogen bonds: charge transfer, resonance assistance and cooperativity. This follows from computational analyses of the structure and bonding in *N*-halo-base pairs and quartets. The objective was to achieve understanding of the nature of resonance-assisted halogen bonds (RAXB): how they resemble or differ from the better understood resonance-assisted hydrogen bonds (RAHB) in DNA. We present an accurate physical model of the RAXB based on molecular orbital theory, which is derived from corresponding energy decomposition analyses and study of the charge distribution. We show that the RAXB arise from classical electrostatic interaction and also receive strengthening from donor–acceptor interactions within the σ -electron system. Similar to the RAHB, there is also a small stabilization by π -electron delocalization. This resemblance leads to prove cooperativity in *N*-halo-guanine quartets, which originates from the charge separation that goes with donor–acceptor orbital interactions in the σ -electron system.

Keywords: Halogen bonds, resonance assistance, cooperativity, MO theory

Introduction

One of the most important intermolecular interactions known are hydrogen bonds (H-bonds). They are responsible for unique features of water, the stability of biological systems such as DNA, and for self-assembly processes in supramolecular chemistry.^{1,2} The nature of this intermolecular interaction has been extensively studied experimentally, as well as theoretically.^{3,4,5} Halogen bonds (X-bonds), although discovered around 150 years ago,⁶ have received considerably less attention. The awareness of the importance of halogen bonds has augmented in the last decades. Nowadays, halogen bonds have applications in various fields of chemistry, such as supramolecular, bio- and inorganic chemistry.^{7,8,9,10,11} This rise in interest has led to various theoretical work to unravel the nature of the halogen bonds, of which some question the differences and similarities with hydrogen bonds.^{12,13,14,15,16,17,18,19} Studies have shown that electrostatic attraction, dispersion, polarization and charge transfer can all contribute significantly to the stability of both H- and X-bonds.^{15,16,20,21,22,23,24} However, halogen bonds are still often considered to have a smaller charge transfer contribution than hydrogen bonds.

With the computational work presented here, we want to demonstrate that H- and X-bonds have equivalent bonding characteristics by comparing trends in interaction energies and deformation densities, both objective criteria. For that reason, we present here the resonance-assisted halogen bonds (RAXB), a phenomenon which has not yet received much attention, and compare these X-bonds to the well-known resonance-assisted hydrogen bonds (RAHB). The latter were proposed by Gilli *et al.*²⁵ and are reinforced by electron delocalization in the π -electron system. In previous work,³ we established theoretically that, for the hydrogen bonds in Watson-Crick DNA base pairs, the electrostatic interactions and charge transfer are of similar importance and that indeed the π electrons provide an additional stabilizing component. These findings have been confirmed by Ziegler and co-workers.²⁶ Furthermore, it has been shown computationally that the synergetic interplay between the delocalization in the π -electron system and the donor–acceptor interactions in the σ -electron system was small, that is, the simultaneous occurrence of the σ and π interactions is only slightly stronger than the sum of these interactions occurring individually.

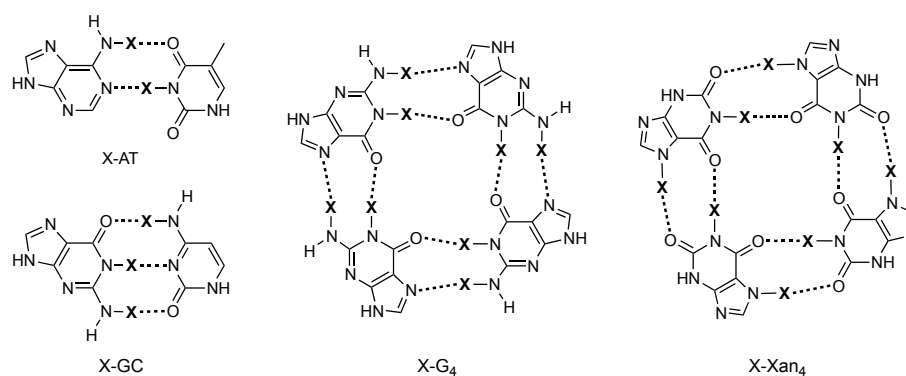


Figure 1. Schematic representation of the Watson-Crick base pairs and the guanine (G_4) and xanthine quartets (Xan_4 ; $X = H$) and the *N*-halo-base pairs (X -AT and X -GC), *N*-halo-guanine quartets (X - G_4) and *N*-halo-xanthine quartets (X - Xan_4) with $X = F, Cl, Br$ or I .

In telomeric DNA, the guanine bases form quadruplexes: a stack of three layers of guanine quartets. The guanine bases in these layers are essentially coplanar and interact through hydrogen bonds. The quadruplexes are furthermore stabilized by the presence of monovalent ions, such as K^+ and Na^+ , between the layers. Intriguingly, the hydrogen-bonding energy of the guanine quartets G_4 (see Figure 1) is known to be more stabilizing than four times the hydrogen-bonding energy of one guanine pair G_2 . Previously, our analyses on telomeric DNA²⁷ revealed that this cooperativity within the H-bonds originates from the charge separation that goes with donor-acceptor orbital interactions in the σ -electron system, and not from the strengthening caused by resonance in the π -electron system.

Cooperativity and resonance assistance have been explored before in the context of halogen-bonded molecular systems, but mainly on small complexes.^{28,29,30,31,32,33,34,35,36,37} We investigated these phenomena for larger aromatic complexes, by substituting the N–H in the natural G_4 quartets with N–X. Chloramines of nucleosides are experimentally known,^{38,39,40,41,42} of which the cytidine and adenosine chloramines are the most stable. In this work, we focus on the halogenated guanine bases to be able to demonstrate for the first time that the X-bonds in an *N*-halo-guanine quartet $X-G_4$ (see Figure 1, with $X = F, Cl, Br$ or I) show the same synergetic enhancement, that is in quantity and nature, as the H-bonds in G_4 . We present an accurate explanation for the physical mechanism of resonance-assisted halogen bonds and the observed cooperativity, which is established in terms of Kohn-Sham molecular orbital (MO) theory,^{43,44,45} and supported by corresponding energy decomposition analyses (EDA)⁴⁶ and Voronoi deformation density (VDD) analyses of the charge distribution⁴⁷ using dispersion-corrected relativistic density functional theory at the ZORA-BLYP-D3(BJ)/TZ2P level of theory.^{48,49} The proof of the intrinsic resemblance between H-bonds and X-bonds will be based on the existence of charge transfer in the X-bonds, which can be directly demonstrated with the cooperativity occurring within $X-G_4$.

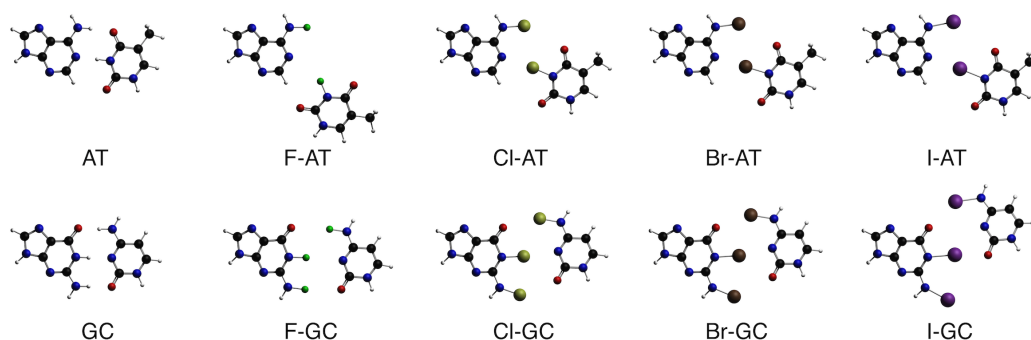


Figure 2. Geometries at ZORA-BLYP-D3(BJ)/TZ2P for the hydrogen- and halogen-bonded AT and GC base pairs in C_s symmetry.

Methods

All calculations were performed with the Amsterdam Density Functional (ADF) program⁵⁰ and QUILD^{51,52} using dispersion-corrected relativistic density functional theory at the ZORA-BLYP-D3(BJ)/TZ2P level for geometry optimizations and energies.^{53,54,55,56} Full computational details are available in the Supplementary Information.

The bond energy ΔE_{bond} of the quartet is defined as:

$$\Delta E_{\text{bond}} = E_{\text{quartet}} - 4 \cdot E_{\text{base}} \quad (1)$$

where E_{quartet} is the energy of the quartet, and E_{base} is the energy of the X-G or X-Xan. The overall bond energy ΔE is made up of two major components:

$$\Delta E_{\text{bond}} = \Delta E_{\text{prep}} + \Delta E_{\text{int}} \quad (2)$$

In this formula, the preparation energy ΔE_{prep} is the amount of energy required to deform the separate bases from their equilibrium structure to the geometry that they acquire in the quartet. The interaction energy ΔE_{int} corresponds to the actual energy change when the prepared bases are combined to form the quartet.

The interaction energy in the hydrogen- and halogen-bonded model systems is examined in the framework of the Kohn-Sham MO model using a quantitative energy decomposition analysis (EDA) into electrostatic interactions, Pauli repulsive orbital interactions, and attractive orbital interactions, to which a term ΔE_{disp} is added to account for the dispersion interactions:⁴³

$$\Delta E_{\text{int}} = \Delta V_{\text{elstat}} + \Delta E_{\text{Pauli}} + \Delta E_{\text{oi}} + \Delta E_{\text{disp}} \quad (3)$$

The term ΔV_{elstat} corresponds to the classical electrostatic interactions between the unperturbed charge distributions of the prepared (i.e. deformed) bases and is usually attractive. The Pauli repulsion ΔE_{Pauli} comprises the destabilizing interactions between occupied orbitals and is responsible for any steric repulsion. The orbital interaction ΔE_{oi} accounts for charge transfer (i.e., donor-acceptor interactions between occupied orbitals on one moiety and unoccupied orbitals on the other, including the HOMO-LUMO interactions) and polarization (empty-occupied orbital mixing on one fragment due to the presence of another fragment).

The orbital interaction energy can be further decomposed into the contributions from each irreducible representation Γ of the interacting system (equation 4) using the extended transition state (ETS) scheme developed by Ziegler and Rauk.⁴⁶ In our planar model systems, this symmetry partitioning allows us to distinguish σ and π interactions:

$$\Delta E_{\text{oi}} = \Delta E_{\text{oi}}^{\sigma} + \Delta E_{\text{oi}}^{\pi} \quad (4)$$

The cooperativity in the hydrogen or halogen bonds in quartets is quantified by comparing ΔE_{int} (i.e., formation of the quartet from four bases in the geometry of the former) with the sum ΔE_{sum} of the individual pairwise interactions for all possible pairs of bases in the quartet, defined as:

$$\Delta E_{\text{sum}} = 4 \cdot \Delta E_{\text{pair}} + 2 \cdot \Delta E_{\text{diag}} \quad (5)$$

Here, ΔE_{pair} is the interaction between two neighboring bases (i.e., the interaction between two doubly hydrogen- or halogen-bonded bases in the geometry of the quartet) and ΔE_{diag} is the interaction between two mutually diagonally oriented bases (i.e., the interaction between two *non*-hydrogen-bonded or *non*-halogen-bonded bases in the geometry of the quartet). The synergy occurring in the quartet is then defined as the difference:

$$\Delta E_{\text{syn}} = \Delta E_{\text{int}} - \Delta E_{\text{sum}} \quad (6)$$

Thus, a negative value of ΔE_{syn} corresponds to a stabilizing cooperative effect, that is, a reinforcement of the quartet stability due to the occurrence of all hydrogen or halogen bonds simultaneously.

Now, we arrive at the analysis of how stacking and cations affect the interaction ΔE_{int} within X-G₄ and X-Xan₄ quartets, in particular, how it affects the cooperativity ΔE_{syn} between hydrogen bonds or halogen bonds. This is achieved by comparing the interaction energy ΔE_{int} for formation of a quartet in a stacking environment (i.e., between the top and bottom G₄ layer of our model stacks) with the formation of the corresponding bare gas-phase quartet. This is done again using the approach of Eqs. 4 and 5. Here, the energy of a quartet X-B₄ and of a base X-B in the stacking environment, are defined as $E_{G_4[X-B_4]G_4} - E_{G_4[]G_4}$ and $E_{G_4[X-B]G_4} - E_{G_4[]G_4}$, respectively, that is, the difference in energy between a stacking environment "occupied" with a central quartet or base and an empty stacking environment. The interaction energy of a quartet in the stacking environment is then given by:

$$\Delta E_{\text{int}} = (E_{G_4[X-B_4]G_4} - E_{G_4[]G_4}) - 4 \cdot (E_{G_4[X-B]G_4} - E_{G_4[]G_4}) \quad (7)$$

Likewise, the sum energy for a quartet in a stacking environment is:

$$\Delta E_{\text{sum}} = 4 \cdot \{(E_{G_4[X-B_2]G_4} - E_{G_4[]G_4}) - 2 \cdot (E_{G_4[X-B]G_4} - E_{G_4[]G_4})\} + 2 \cdot \{(E_{G_4[X-B/X-B]G_4} - E_{G_4[]G_4}) - 2 \cdot (E_{G_4[X-B]G_4} - E_{G_4[]G_4})\}, \quad (8)$$

which contains, in analogy to equation (5), four times the hydrogen- or halogen-bonded pair interaction ΔE_{pair} in the stacking environment (first line) and twice the diagonal base–base interaction ΔE_{diag} in the stacking environment. The effect of stacking and potassium cations can be easily derived from equations (7) and (8) by substituting “G₄[]G₄” with “G₄K⁺[]K⁺G₄”, which includes the cations in the environment.

Results and Discussion

B-DNA

Before starting our analysis of the quadruplexes, we investigated the nature of the bonding in the halogen-substituted Watson-Crick base pairs. From earlier studies,⁵⁷ it is known that the halogen-bonded X-AT and X-GC are weaker bound than the natural AT and GC (see Table 1). Indeed, we found that the fluorinated Watson-Crick base pairs are almost unbound ($-1.4 \text{ kcal mol}^{-1}$ when symmetry constraints are applied, without constraints no halogen-bonding interactions are present), whereas the halogen bonds in the iodine-substituted AT and GC pairs amount to $-10.7 \text{ kcal mol}^{-1}$ and $-17.3 \text{ kcal mol}^{-1}$, respectively. Furthermore, it has been shown that hydrogen and halogen bonds are governed by similar bonding mechanisms.^{15,16} We analyzed the X- and H-bonds for these dimers in the conceptual framework provided by the Kohn-Sham molecular orbital model through a decomposition of the interaction energy (ΔE_{int}) into the classical electrostatic interactions (ΔV_{elstat}), the attractive orbital interactions comprising charge transfer and polarization (ΔE_{oi}), dispersion interactions (ΔE_{disp}) and the Pauli repulsive orbital interactions between closed shells (ΔE_{pauli}).⁴³ It appears that in both the X- and H-bonded base pairs, the bonding orbital interactions associated with X- or H-bonding and the electrostatic attraction are of comparable magnitude (see Table 1). For clarity, we like to stress that the ΔV_{elstat} term within this work is computed from the complete charge distributions of both fragments, and therefore has no direct relation with molecular electrostatic potential plots, which are often provided in studies on hydrogen bonds, halogen bonds and similar interactions. Halogen bonds are typically described as arising from a positive region, the σ -hole, appearing at the halogen atom in such molecular electrostatic potential plots.^{18,58,59,60} Often, but not always, a correlation is found between the σ -hole and the halogen bond strength.^{20,21,23}

Similar to the H-bonded bases, the largest contribution to the orbital interactions in the X-bonds comes from the σ electrons: resonance assistance by π -electron delocalization plays only a small role. The dispersion interaction is smaller than the orbital and electrostatic interaction. In line with previous findings,¹⁶ we find that the strengthening from the fluorine bonds to the iodine bonds follows from an increase in all bonding components.

The X-bonds in the halogen-substituted base pairs differ geometrically from the H-bonds in the natural DNA base pairs. The larger halogen atoms do not pair perfectly with the opposite base. This effect becomes more pronounced from chlorine- to iodine-substituted base pairs, as the halogen atoms are too large to fit next to each other (see Figure 2).

Table 1. Bond energy analyses (kcal mol⁻¹) for natural and halogenated Watson-Crick base pairs.^[a]

	ΔE	ΔE_{prep}	ΔE_{int}	ΔE_{elstat}	ΔE_{Pauli}	ΔE_{oi}	$\Delta E_{\text{oi}}^{\sigma}$	$\Delta E_{\text{oi}}^{\pi}$	ΔE_{disp}
AT	-16.7	1.9	-18.5	-32.0	40.1	-21.2	-19.6	-1.6	-5.4
F-AT	-1.4	0.1	-1.4	-1.8	3.7	-1.5	-1.4	-0.2	-1.8
Cl-AT	-6.3	0.4	-6.7	-13.0	19.9	-8.9	-8.5	-0.4	-4.8
Br-AT	-9.7	1.3	-11.0	-22.9	33.7	-15.6	-14.7	-0.9	-6.3
I-AT	-10.7	2.0	-12.7	-24.7	35.4	-16.1	-15.1	-1.0	-7.3
GC	-30.4	3.5	-34.0	-47.7	51.9	-31.9	-27.4	-4.5	-6.3
F-GC	-1.4	0.1	-1.5	-1.3	4.0	-2.1	-1.8	-0.3	-2.1
Cl-GC	-9.1	0.6	-9.7	-14.2	19.3	-8.6	-7.7	-0.8	-6.2
Br-GC	-12.9	1.2	-14.1	-23.5	32.5	-15.2	-13.9	-1.3	-7.9
I-GC	-17.3	2.5	-19.7	-28.7	38.3	-21.5	-19.5	-2.0	-7.9

[a] Energies computed at ZORA-BLYP-D3(BJ)/TZ2P in C_s symmetry for base pair and base. The bond energies for the fully optimized base pairs and bases differ slightly (see SI, Table S1).

G-DNA

After the establishment of the large contribution of the σ orbital interactions to the bonding of the halogen-substituted base pairs, the investigation was extended to telomeric DNA. The *N*-halo-quartets have, as is the case for the natural guanine and xanthine quartets, an S_4 or C_4 symmetric global minimum structure. However, in the quadruplex, which is the natural occurring structure of guanine quartets, computations showed an almost planar middle layer for the Br- G_4 quartet, which allows for favorable dispersion interactions (see Figure 3a). The Br- G_4 quartet is only 2.3 kcal mol⁻¹ lower in energy in the geometry it acquires in the quadruplex $G_4\text{-K}^+\text{-[Br-}G_4\text{]-K}^+\text{-}G_4$, than in a C_{4h} geometry. Therefore, the quartets have been optimized and analyzed in C_{4h} symmetry to enable the separation between the σ - and π -orbital interactions.

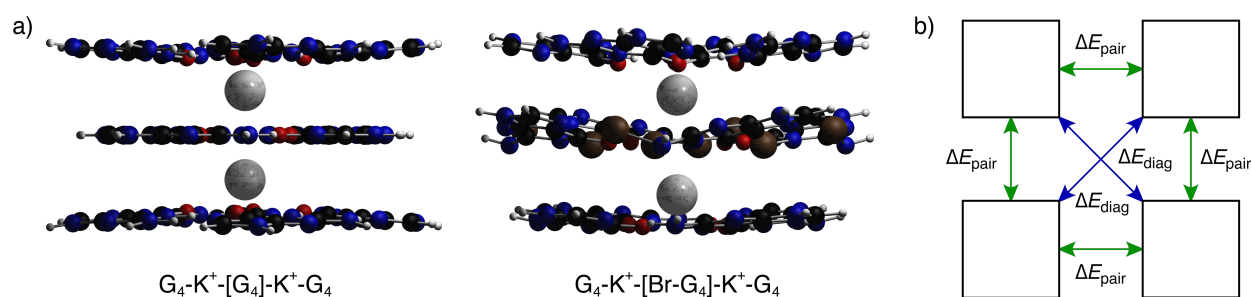


Figure 3. a) Structures of stacked $G_4\text{-K}^+\text{-[G}_4\text{]-K}^+\text{-}G_4$ (left) and $G_4\text{-K}^+\text{-[Br-}G_4\text{]-K}^+\text{-}G_4$ (right) in C_4 symmetry at ZORA-BLYP-D3(BJ)/TZ2P. b) Definition of pairwise interaction-energy terms (arrows) in quartet of DNA bases (squares).

The computational experiment to prove the existence of covalency as bonding component in the *N*-halo-quartets started with the comparison of the halogenated guanine and xanthine quartets as presented in Figure 1 and 4. We recall from earlier work²⁷ that guanine quartets (G_4) are more strongly bound than xanthine quartets (Xan_4), despite the fact that they have the same number of hydrogen bonds. This is ascribed to a cooperativity effect in the former. The interaction energy of G_4 amounts to $-90.6 \text{ kcal mol}^{-1}$ whereas ΔE_{int} of Xan_4 is only $-73.4 \text{ kcal mol}^{-1}$ (see Table 2). Interestingly, the same is true for the Cl-, Br- or I-substituted quartets. The interaction energy of $X-G_4$ for $X = \text{Cl}, \text{Br}$ and I is, respectively, $-13.4 \text{ kcal mol}^{-1}$, $-35.0 \text{ kcal mol}^{-1}$ and $-46.8 \text{ kcal mol}^{-1}$ stronger than ΔE_{int} of the analogous $X-Xan_4$.

The cooperativity in the X-bonds is proven by comparing the interaction energy ΔE_{int} of the $X-G_4$ with the sum of pairwise interactions, ΔE_{sum} . The sum of pairwise interactions is obtained by adding four times the pair interaction ΔE_{pair} , to two times the diagonal interactions, ΔE_{diag} (see Figure 3b). The synergy ($\Delta E_{\text{int}} - \Delta E_{\text{sum}}$) for $\text{Br-}G_4$ and $\text{I-}G_4$ amounts to $-23.5 \text{ kcal mol}^{-1}$ and $-24.9 \text{ kcal mol}^{-1}$, which is even stronger than for the natural G_4 ($-20.9 \text{ kcal mol}^{-1}$).

The experiments were extended to the quadruplexes (Figure 3a). The synergy is barely affected by the molecular environment and non-planarity: for G_4 and $\text{Br-}G_4$ quartets in the quadruplexes it is $-17.9 \text{ kcal mol}^{-1}$ and $-17.7 \text{ kcal mol}^{-1}$ respectively (see equation (7) and (8) for the calculation of the synergy in the quadruplexes). These computational experiments confirm the intrinsic resemblance between halogen and hydrogen bonds.

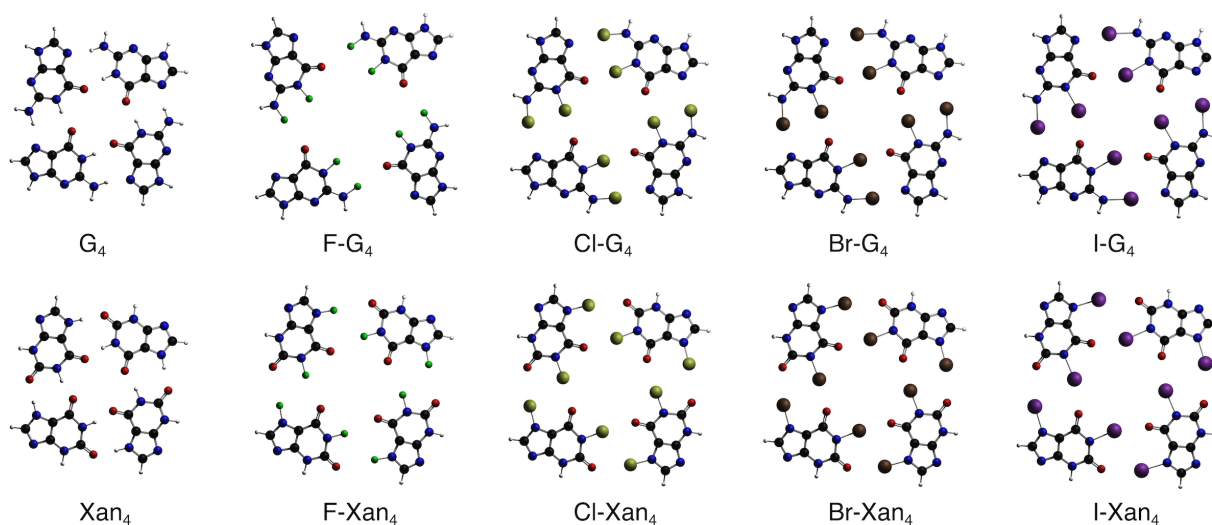


Figure 4. Geometries at ZORA-BLYP-D3(BJ)/TZ2P for the hydrogen- and halogen-bonded $X-G_4$ and $X-Xan_4$ quartets in C_{4h} symmetry.

These quadruplexes can be further analyzed. The stacking interaction in the $G_4-K^+-[G_4]-K^+-G_4$ quadruplex is smaller than in the $G_4-K^+-[Br-G_4]-K^+-G_4$ quadruplex. The stacking between the three G_4 layers in $G_4-[G_4]-G_4$ (no K^+ present) amounts to $-66.2 \text{ kcal mol}^{-1}$, and between the G_4 , $\text{Br-}G_4$ and G_4 in $G_4-[Br-G_4]-G_4$ to $-72.6 \text{ kcal mol}^{-1}$. When K^+ is present, the interaction between the potassium cations and the stacked quartets is larger for $G_4-K^+-[G_4]-K^+-G_4$ ($-205.6 \text{ kcal mol}^{-1}$)

than for the $G_4\text{-K}^+[\text{Br-G}_4]\text{-K}^+\text{-G}_4$ (-176.9 kcal mol $^{-1}$). The smaller interaction with the cations in $G_4\text{-K}^+[\text{Br-G}_4]\text{-K}^+\text{-G}_4$ can be attributed to the larger distance between the K^+ ions and the oxygen atoms of the central quartet (3.8 to 3.9 Å). In the $G_4\text{-K}^+[\text{G}_4]\text{-K}^+\text{-G}_4$ quadruplex, the oxygen atoms of the central quartet are much closer to the K^+ ions: the distance is only 2.9 Å. The additional lone pairs on the bromines probably do not contribute to the overall stability of the K^+ -mediated complex as they are more than 4 Å from K^+ .

Table 2. Interaction energy analysis (kcal mol $^{-1}$) of G_4 and Xan_4 quartets.^[a]

Environment	Quartet	Symmetry	$\Delta E_{\text{int}}^{[b]}$	$\Delta E_{\text{diag}}^{[b]}$	$\Delta E_{\text{pair}}^{[b]}$	$\Delta E_{\text{sum}}^{[b]}$	Synergy ^[b]
gas phase	G_4	C_{4h}	-90.6	-1.9	-16.5	-69.7	-20.9
	F- G_4	C_{4h}	-3.1	+0.1	-0.7	-2.4	-0.7
	Cl- G_4	C_{4h}	-39.5	-0.1	-7.5	-30.3	-9.2
	Br- G_4	C_{4h}	-77.5	-0.6	-13.2	-54.0	-23.5
	I- G_4	C_{4h}	-97.8	-1.3	-17.6	-72.9	-24.9
	Xan_4	C_{4h}	-73.4	-0.2	-17.9	-71.9	-1.5
	F- Xan_4	C_{4h}	-2.9	+0.4	-0.8	-2.4	-0.5
	Cl- Xan_4	C_{4h}	-26.1	+0.1	-6.5	-25.7	-0.4
	Br- Xan_4	C_{4h}	-42.5	-0.1	-10.4	-41.7	-0.8
	I- Xan_4	C_{4h}	-51.0	-0.3	-12.4	-50.3	-0.8
$G_4\text{-}[\]\text{-G}_4$	G_4	C_4	-89.2	-1.9	-17.4	-73.4	-15.8
	Br- G_4	C_4	-56.0	-0.5	-10.6	-43.4	-12.7
$G_4\text{-K}^+\text{-}[\]\text{-K}^+\text{-G}_4$	G_4	C_4	-72.7	+0.6	-14.0	-54.8	-17.9
	Br- G_4	C_4	-47.0	+0.3	-7.5	-29.3	-17.7

[a] computed at ZORA-BLYP-D3(BJ)/TZ2P. See Figure 3b and Equations (5) to (8).

For the natural quadruplexes, the cooperativity has been shown to originate from the charge separation that goes with donor–acceptor interactions in the σ -electron system from N and O lone-pair orbitals on one guanine to $\sigma_{\text{N-H}}^*$ acceptor orbitals on the other guanine.²⁷ To trace the origin of the cooperativity in halogen-substituted guanine quartets, we have followed the same procedure: we constructed X-G_4 by taking one of the *N*-halo-guanine bases in the quartet and stepwise adding the other three *N*-halo-guanine bases (always in the geometry of X-G_4), i.e., $\text{X-G} + \text{X-G} = \text{X-G}_2$, $\text{X-G}_2 + \text{X-G} = \text{X-G}_3$ and $\text{X-G}_3 + \text{X-G} = \text{X-G}_4$ (see Figure 5a and Table S3). This stepwise approach enables us to examine accurately why, and at which point, cooperativity begins to show up. Except for F- G_4 , which is almost unbound, the *N*-halo-quartets show a trend similar to the natural G_4 . For example, the interaction energy in I- G_2 amounts to -17.6 kcal mol $^{-1}$, between I- G_2 and I-G it is already larger, -24.4 kcal mol $^{-1}$ and the interaction energy for closure of the quartet by the formation of four halogen bonds (that is between I- G_3 and I-G) is -55.8 kcal

mol^{-1} . Thus, the cooperative effect increases systematically and monotonically as the X-G_{n-1} fragment becomes larger. A similar computational experiment with X-Xan_4 quartets reveals no cooperativity at all (see Table S4). As both quartets have π electrons, this outcome points towards the σ -electron system as the responsible factor for the cooperativity in X-G_4 .

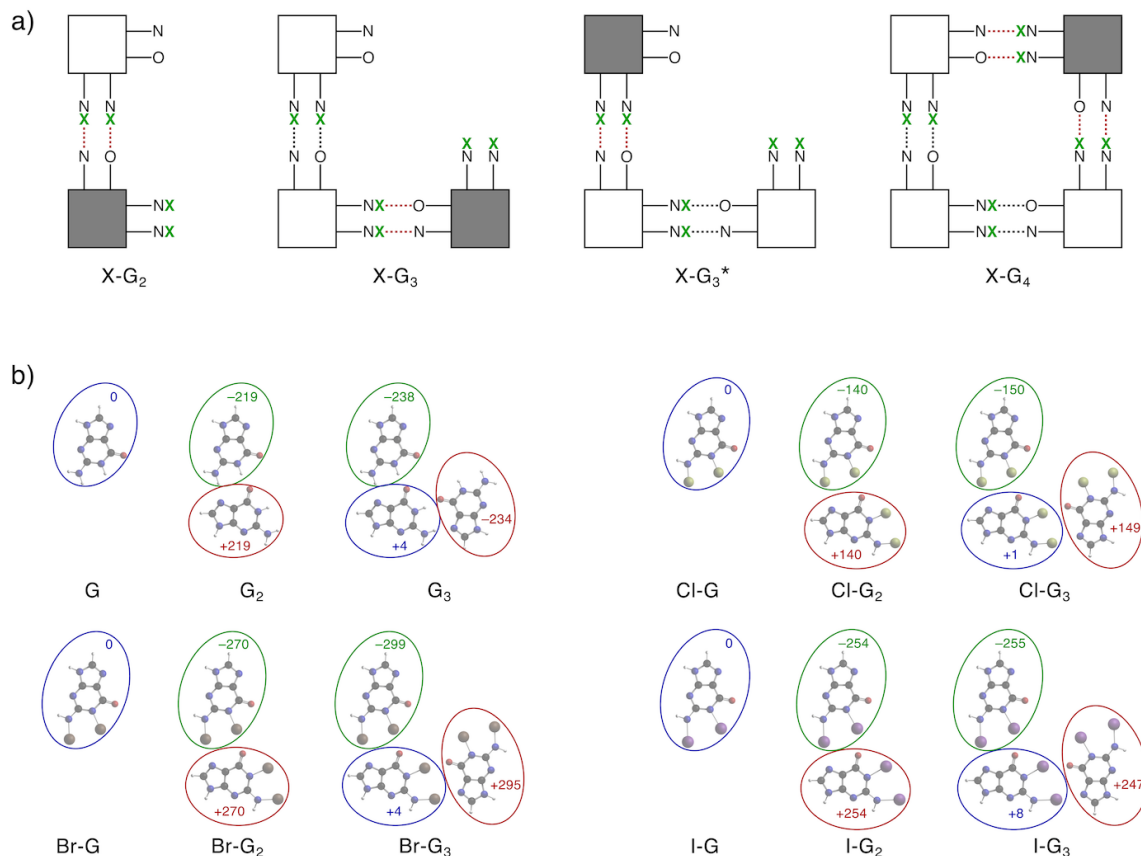


Figure 5. a) Formation of X-G_4 quartet in three steps: $\text{X-G} + \text{X-G} = \text{X-G}_2$; $+ \text{G} = \text{G}_3^*$; $+ \text{X-G} = \text{X-G}_4$. b) VDD charges (milli-electrons) computed at ZORA-BLYP-D3(BJ)/TZ2P for fragments of the hydrogen-bonded G_4 and halogen-bonded X-G_4 quartets in C_{4h} symmetry.

To investigate whether the cooperativity in N -halo-guanine quartets is caused by a similar mechanism as in the natural guanine quartets, we subjected the total interaction energy, $\Delta E_{\text{int}} = \Delta E_{\text{int}}(\text{X-G}_2) + \Delta E_{\text{int}}(\text{X-G}_3) + \Delta E_{\text{int}}(\text{X-G}_4)$ to an energy decomposition analysis. The synergy in each energy component, for example ΔE_{oi} , is now defined, in analogy to Figure 3b and 5a, as the difference between $\Delta E_{\text{oi}}(\text{X-G}_2) + \Delta E_{\text{oi}}(\text{X-G}_3) + \Delta E_{\text{oi}}(\text{X-G}_4)$ and the sum of the corresponding energy component in the pairwise interactions, i.e., $4 \cdot \Delta E_{\text{pair,oi}} + 2 \cdot \Delta E_{\text{diag,oi}}$. The energy decomposition analyses show that there are two main contributions to this synergy: (i) the synergy in the electrostatic attraction of $-3.8 \text{ kcal mol}^{-1}$, $-8.3 \text{ kcal mol}^{-1}$ and $-6.3 \text{ kcal mol}^{-1}$ for Cl-G_4 , Br-G_4 and I-G_4 , respectively; and (ii) the much stronger synergy in the orbital interactions of $-5.8 \text{ kcal mol}^{-1}$, $-15.6 \text{ kcal mol}^{-1}$ and $-20.0 \text{ kcal mol}^{-1}$ for Cl-G_4 , Br-G_4 and I-G_4 , respectively. The latter originates almost exclusively from the charge-transfer orbital interactions in the σ -electron system (-5.0 , -13.7 and $-18.3 \text{ kcal mol}^{-1}$ for Cl-G_4 , Br-G_4 and I-G_4 , respectively), with

only minor contributions stemming from synergy in the resonance assistance of the π -electron system (see Table S3). Therefore, one can conclude that the cooperativity leading to the enhanced stability of the X-G₄ quartets does *not* stem from resonance assistance.

The synergy in the σ -electron system is, for Br-G₄ and I-G₄, even larger than for the natural G₄, for which it amounts to -8.2 kcal mol⁻¹. This is, again, in good agreement with previous results on halogen-bonded complexes,^{16,20} where it was shown that, upon going from fluorine to iodine bonds, the orbital interactions become more important due to a lower acceptor orbital on the halogen-donating fragment. This can lead to an even larger covalent character for halogen bonds than for the analogous hydrogen bonds, and consequently a stronger cooperative effect.

Analysis of the electron density confirms this picture, and provides a straightforward explanation for the cooperativity in halogen-bonded quartets: the donor–acceptor orbital interactions associated with the ΔE_{oi}^{σ} term, induce a charge separation, which in turn enhances both the orbital interactions and the electrostatic attraction with an additional *N*-halo-guanine base. The σ donor–acceptor interactions between antibonding acceptor orbitals of the N–X moiety on one X-G and N and O lone-pair orbitals on a second X-G lead to a slight but important charge transfer in the resulting X-G₂ complex (see Figure 5b). The former X-G base builds up a net negative charge of -140 , -270 and -254 milli-electrons for X = Cl, Br, and I respectively, and the latter base builds up a net positive charge of $+140$, $+270$, $+254$ milli-electrons, respectively (with slightly less charge accumulation for X = I due to back-donation, see SI). As a consequence, the orbitals in the former Cl-G base in Cl-G₂ are destabilized due to the net negative charge, making the N and O lone-pair orbitals better partners in the donor–acceptor interactions with a third X-G base (see Figure 6). The energy of the N and O lone-pair orbital σ_{HOMO} rises from -6.3 eV in Cl-G to -5.5 eV in Cl-G₂. Also for the fragments of Br-G₄ and I-G₄ a rise of about 1 eV of the σ_{HOMO} is observed upon going from X-G to X-G₂. (see Table S5 and S6). Likewise, the orbitals on the other X-G base in X-G₂ are stabilized by the net positive charge, making the $\sigma_{\text{N-X}}^*$ orbitals better partners for donor–acceptor interactions with a third X-G base (see Figure 6). In the case of Cl-G, for example, the energy of the N–Cl anti-bonding acceptor orbital (σ_{LUMO}) decreases from -3.2 eV in Cl-G to -3.5 eV in Cl-G₂. These findings are further strengthened by analyses of the orbital populations, which indicate steadily stronger donor–acceptor interactions occurring in X-G₂, X-G₃ and X-G₄, as well as from chlorine- to bromine- to iodine-bonding guanine fragments. For Br-G₄, for example, the combined population of both $\sigma_{\text{N-Br}}^*$ acceptor orbitals increases monotonically from 0.20 electrons when two Br–G fragments interact, to 0.22 and 0.26 electrons when the third and fourth fragment are added, respectively.

Thus, cooperativity becomes more pronounced every time an additional X-G base is added because such an addition will amplify the charge separation, and thereby the donor–acceptor interactions (see Figures 5-6 and Table S5–S6). The strongest synergy is found when the fourth and last *N*-halo-guanine base of X-G₄ is introduced because this quenches the electrostatically unfavorable charge separation in the X-G₃ fragment.

Conclusions

The computational experiment presented in this work, in which we evoked cooperativity in hydrogen- and halogen-bonded compounds, demonstrates clearly the resemblance between halogen and hydrogen bonds. The equivalence between RAHB and RAXB in natural and *N*-haloguanine quartets is proven by the existence of resonance assistance in the π -electron system and charge transfer that goes with donor–acceptor orbital interactions in the σ -electron system from N and O lone-pair orbitals on one X-G base to $\sigma^*_{\text{N-H}}$ or $\sigma^*_{\text{N-X}}$ acceptor orbitals on the other X-G base. Thus, whereas the covalency in hydrogen bonds was previously demonstrated by the cooperativity in natural G_4 , the even stronger charge transfer present in halogen bonds has now been demonstrated in a similar way, by revealing an even stronger cooperative effect in *N*-haloguanine quartets. Notably, this is achieved using unambiguous quantities, namely the interaction energy and the density deformation. A physical interpretation of the results has been accomplished using Kohn-Sham MO theory, supported by a quantitative interaction energy decomposition scheme.

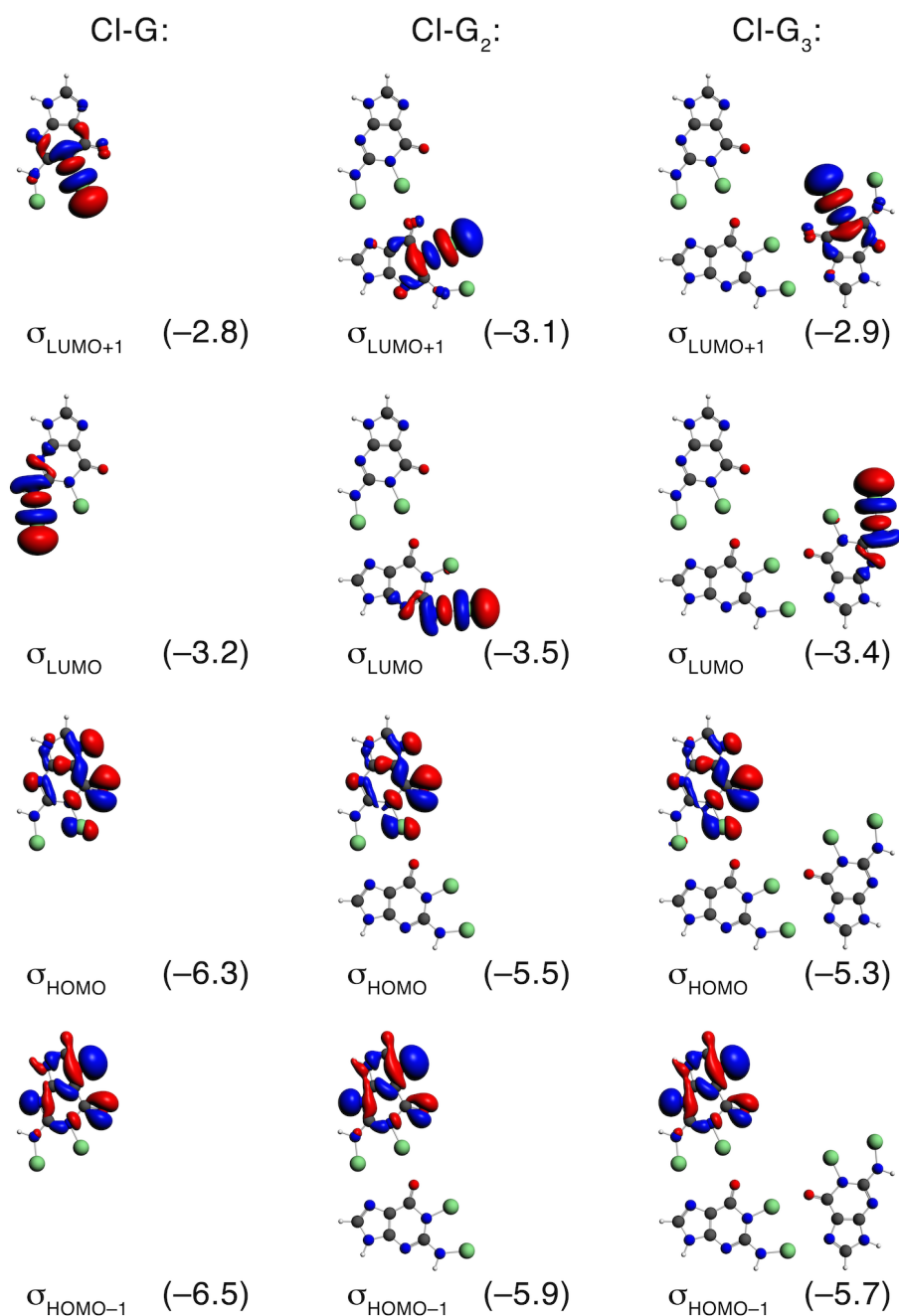


Figure 6. Electron-donating highest occupied molecular orbitals (HOMOs) and electron-accepting lowest unoccupied molecular orbitals (LUMOs) with their energies (eV) in the σ -electron system on the fragments of the C_{4h} -symmetric Cl-G₄ quartet.

Acknowledgements

We thank the National Research School Combination - Catalysis and the Netherlands Organization for Scientific Research (NWO-CW and NWO-EW) for financial support.

Additional information

Supplementary information contains Cartesian coordinates of all molecular species, full computational details and additional numerical results.

References

1. G. A. Jeffrey, *An introduction to hydrogen bonding*, Oxford Univ. Press, New York, 1997.
2. G. R. Desiraju and T. Steiner, *The weak hydrogen bond in structural chemistry and biology*, Oxford Univ. Press, New York, 1999.
3. C. Fonseca Guerra, F. M. Bickelhaupt, J. G. Snijders and E. J. Baerends, *Chem. Eur. J.*, 1999, **5**, 3581-3594.
4. S. Scheiner, *Hydrogen Bonding. A Theoretical Perspective*, Oxford Univ. Press, New York, 1997.
5. H. Umeyama and K. Morokuma, *J. Am. Chem. Soc.*, 1977, **99**, 1316-1332.
6. F. Guthrie, *J. Chem. Soc.*, 1863, **16**, 239-244.
7. A. Priimagi, G. Cavallo, P. Metrangolo and G. Resnati, *Acc Chem Res.*, 2013, **46**, 2686-2695.
8. G. Cavallo, P. Metrangolo, T. Pilati, G. Resnati, M. Sansotera and G. Terraneo, *Chem Soc Rev.*, 2010, **39**, 3772-3783.
9. Y. Lu, Y. Liu, Z. Xu, H. Li, H. Liu and W. Zhu, *Expert Opin. Drug Discov.*, 2012, **7**, 375-383.
10. R. Wilcken, M. O. Zimmermann, A. Lange, A. C. Joerger and F. M. Boeckler, *J. Med. Chem.*, 2013, **56**, 1363-1388.
11. L. Brammer, G. M. Espallargas and S. Libri, *CrystEngComm*, 2008, **10**, 1712-1727.
12. P. Politzer, J. S. Murray and P. Lane, *Int. J. Quantum Chem.*, 2007, **107**, 3046-3052.
13. P. Cimino and M. Pavone, *J. Phys. Chem. A*, 2007, **111**, 8482-8490.
14. I. Alkorta, F. Blanco and M. Solimannejad, *J. Phys. Chem. A*, 2008, **112**, 10856-10863.
15. M. Palusiak, *J. Mol. Struct. THEOCHEM.*, 2010, **945**, 89-92.

16. L. P. Wolters and F. M. Bickelhaupt, *ChemistryOpen*, 2012, **1**, 96-105.
17. S. V. Rosokha, C. L. Stern and J. T. Ritzert, *Chem. Eur. J.*, 2013, **19**, 8774-8788.
18. P. Politzer, J. S. Murray and T. Clark, *Phys. Chem. Chem. Phys.*, 2013, **15**, 11178-11189.
19. S. Scheiner, *Acc. Chem. Res.*, 2013, **46**, 280-288.
20. S. M. Huber, E. Jimenez-Izal, J. M. Ugalde and I. Infante, *Chem. Commun.*, 2012, **48**, 7708-7710.
21. S. M. Huber, J. D. Scanlon, E. Jimenez-Izal, J. M. Ugalde and I. Infante, *Phys. Chem. Chem. Phys.*, 2013, **15**, 10350-10357.
22. B. Pinter, N. Nagels, W. A. Herrebout and F. De Proft, *Chem. Eur. J.*, 2013, **19**, 519-530.
23. A. J. Stone, *J. Am. Chem. Soc.*, 2013, **135**, 7005-7009.
24. P. Politzer and J. S. Murray, *ChemPhysChem*, 2013, **14**, 278-294.
25. G. Gilli, F. Bellucci, V. Ferretti and V. Bertolasi, *J. Am. Chem. Soc.*, 1989, **111**, 1023-1028.
26. R. Kurczab, M. P. Mitoraj, A. Michalak and T. Ziegler, *Phys. Chem. A*, 2010, **114**, 8581-8590.
27. C. Fonseca Guerra, H. Zijlstra, G. Paragi and F. M. Bickelhaupt, *Chem. Eur. J.*, 2011, **17**, 12612-12622.
28. R. D. Parra, *Comput. Theor. Chem.*, 2012, **998**, 183-192.
29. S. J. Grabowski and E. Bilewicz, *Chem. Phys. Lett.*, 2006, **427**, 51-55.
30. R. W. Góra, M. Maj and S. J. Grabowski, *Phys. Chem. Chem. Phys.*, 2013, **15**, 2514-2522.
31. I. Alkorta, F. Blanco and J. Elguero, *Struct. Chem.*, 2009, **20**, 63-71.
32. I. Alkorta, F. Blanco, P. M. Deyà, J. Elguero, C. Estarellas, A. Frontera and D. Quiñonero, *Theor. Chem. Acc.*, 2009, **126**, 1-14.
33. J. George, V. L. Deringer and R. Dronskowski, *J. Phys. Chem. A*, 2014, **118**, 3193-3200.
34. S. A. C. McDowell, *Chem. Phys. Lett.*, 2014, **598**, 1-4.
35. M. Domagala and M. Palusiak, *Comp. Theor. Chem.*, 2014, **1027**, 173-178.
36. X. C. Yan, P. Schyman and W. L. Jorgensen, *J. Phys. Chem. A*, 2014, **118**, 2820-2826.
37. L. Albrecht, R. J. Boyd, O. Mó and M. Yáñez, *J. Phys. Chem. A*, 2014, **118**, 4205-4213.
38. C. L. Hawkins, M. Davies, *J. Chem. Res. Toxicol.*, 2001, **14**, 1071-1081.
39. J. P. Gould, J. T. Richards, M. G. Miles, *Water Res.*, 1984, **18**, 991-999.
40. A. Ohkubo, Y. Noma, K. Aoki, H. Tsunoda, K. Seio, M. Sekine, *J. Org. Chem.*, 2009, **74**, 2817-2823.
41. Y. Kawai, Y. Matsui, H. Kondo, H. Morinaga, K. Uchida, N. Miyoshi, Y. Nakamura, T. Osawa, *Chem. Res. Toxicol.*, 2008, **21**, 1407-1414.
42. M. Ikehara, Y. Ogiso, T. Maruyama, *Chem. Pharm. Bull.*, 1977, **25**, 575-578.

43. F. M. Bickelhaupt and E. J. Baerends, *Rev. Comput. Chem.* Vol. 15 (eds Lipkowitz, K. B. and Boyd, D. B.), Wiley-VCH, New York, 2000, pp. 1-86.
44. R. Stowasser, R. Hoffmann, *J. Am. Chem. Soc.*, 1999, **121**, 3414–3420.
45. E. J. Baerends, O. V. Gritsenko, R. Van Meer, *Phys. Chem. Chem. Phys.*, 2013, **15**, 16408–16425.
46. T. Ziegler and A. Rauk, *Inorg Chem.*, 1979, **18**, 1558-1565.
47. C. Fonseca Guerra, J.-W. Handgraaf, E. J. Baerends and F. M. Bickelhaupt, *J. Comput. Chem.*, 2004, **25**, 189-210.
48. E. J. Baerends, *et al.* ADF2012, <http://www.scm.com/>
49. C. Fonseca Guerra, T. van der Wijst, J. Poater, M. Swart and F. M. Bickelhaupt, *Theor. Chem. Acc.*, 2010, **125**, 245–252.
50. G. te Velde, F. M. Bickelhaupt, S. J. A. van Gisbergen, C. Fonseca Guerra, E. J. Baerends, J. G. Snijders and T. Ziegler, *J. Comput. Chem.*, 2001, **22**, 931-967.
51. M. Swart and F. M. Bickelhaupt, *Int. J. Quantum Chem.*, 2006, **106**, 2536-2544.
52. M. Swart and F. M. Bickelhaupt, *J. Comput. Chem.*, 2008, **29**, 724-734.
53. E. van Lenthe, E. J. Baerends and J. G. Snijders, *J. Chem. Phys.*, 1994, **101**, 9783-9792.
54. E. van Lenthe and E. J. Baerends, *J. Comput. Chem.*, 2003, **24**, 1142-1156.
55. S. Grimme, S. Ehrlich and L. Goerigk, *J. Comput. Chem.*, 2011, **32**, 1456-1465.
56. E. R. Johnson and A. D. Becke, *J. Chem. Phys.*, 2005, **123**, 024101-024107.
57. A. J. Parker, J. Stewart, K. J. Donald and C. A. Parish, *J. Am. Chem. Soc.*, 2012, **134**, 5165-5172.
58. A. C. Legon, *Angew. Chem. Int. Ed.*, 1999, **38**, 2686-2714.
59. T. Brinck, J. S. Murray, P. Politzer, *Int. J. Quant. Chem.*, 1992, **44**, 57-64.
60. T. Clark, M. Hennemann, J. Murray, P. Politzer, *J. Mol. Model.*, 2007, **13**, 291-296.